Dense spectrum of resonances and particle capture in a near-black-hole metric

V. V. Flambaum and G. H. Gossel

School of Physics, University of New South Wales, Sydney 2052, Australia

G. F. Gribakin

School of Mathematics and Physics, Queen's University, Belfast BT7 1NN, Northern Ireland, United Kingdom

We show that a quantum scalar particle in the gravitational field of a massive body of radius R which slightly exceeds the Schwarzschild radius r_s, possesses a dense spectrum of narrow resonances. Their lifetimes and density tend to infinity in the limit $R \rightarrow r_s$. We determine the cross section of the particle capture into these resonances and show that it is equal to the absorption cross section for a Schwarzschild black hole. Thus, a nonsingular static metric acquires black-hole properties before the actual formation of a black hole.

I. INTRODUCTION

The static Schwarzschild metric for a compact massive spherical body (i.e., a black hole) has a coordinate singularity at the event horizon $r = r_s$, where r_s is the Schwarzschild radius. The absorption cross section by this object is usually calculated by assuming a purely ingoing-wave boundary condition at $r \rightarrow r_s$ [1–7]. In particular, for a massless scalar particle Unruh showed that $\sigma_a = 4\pi r_s^2$ at zero energy [3]. More recently Kuchiev continued the wave function analytically across the event horizon and found a nonzero gravitational reflection coefficient $\mathcal{R}$ from $r = r_s$ [8,9], which results in $\sigma_a = 0$ at zero energy. Subsequently, the absorption cross section was determined for an arbitrary reflection coefficient $\mathcal{R}$ which may, in principle, include gravitational, electromagnetic, and other interactions [10].

In this paper we consider the scattering problem for a massless scalar particle in a nonsingular metric of a massive body of radius $R > r_s$. We find that in the limit $R \rightarrow r_s$, an increasingly dense spectrum of narrow *resonances* emerges in the system. These quasistationary states exist in the interior of the body of radius R, which resembles a ''resonant cavity.'' (Note that these resonances are different from the orbital resonances which exist outside a black hole, see, e.g., Refs. [11–17].)

For $R \rightarrow r_s$ both the resonance energy spacing D and their width γ tend to zero, while their ratio remains finite, e.g., $\gamma/D \simeq 2\varepsilon^2 r_s^2/\pi$ for small energies ε. (We use units where $\hbar = c = 1$.) This allows one to define the cross section for particle capture into these long-lived states in the spirit of the optical model [18], by averaging over a small energy interval containing many resonances. Note that this capture emerges in a purely potential scattering problem, without any absorption introduced *a priori*. Somewhat unexpectedly, the capture cross section turns out to be equal to the cross section obtained by assuming total absorption at the event horizon (i.e., for the reflection

coefficient $\mathcal{R} = 0$). In particular, in the zero-energy limit our result coincides with Unruh's absorption cross section for a black hole.

It is worth noting that the quantum scattering delay time associated with the resonances, i.e., their lifetime $t = \hbar/\gamma$, is much longer than the classical gravitation dilation time. The resonance lifetime tends to infinity in the limit $R \rightarrow r_s$, and the resonance capture becomes equivalent to absorption (i.e., the particle does not come out during finite time). Therefore, we observe a smooth, physical transition to the black-hole limit with typical black-hole gravitational properties emerging for a nonsingular static metric prior to the actual formation of the black hole. We should add that in the case of finite-mass particles this picture is complemented by a dense spectrum of the gravitationally *bound* states located in the range $r < R$, see, e.g., Refs. [14,19]. Here too the spectrum becomes infinitely dense in the limit $R \rightarrow r_s$, and the lowest level approaches $\varepsilon = 0$ (i.e., the binding energy is $-mc^2$).

We note that quantum effects (including the famous Hawking radiation) are negligible for the star-mass black holes. Therefore, we do not aim to consider real stars (see, e.g., [20]). In the present work we consider the theoretical question of how quantum effects manifest themselves when a metric approaches the black-hole metric.

II. SCATTERING BY STATIC SPHERICALLY SYMMETRIC BODY

A. Exterior solution

The Klein-Gordon equation for a scalar particle of mass m in a curved space-time with the metric $g_{\mu\nu}$ is

$$\partial_\mu(\sqrt{-g}g^{\mu\nu}\partial_\nu\Psi) + \sqrt{-g}m^2\Psi = 0. \tag{1}$$

Outside a spherically symmetric, nonrotating body of mass M and radius R the metric is given by the Schwarzschild solution

$$ds^2 = \left(1 - \frac{r_s}{r}\right)dt^2 - \left(1 - \frac{r_s}{r}\right)^{-1}dr^2 - r^2 d\Omega^2, \quad (2)$$

where $r_s = 2GM$, G is the gravitational constant, and $d\Omega^2 = d\theta^2 + \sin^2\theta d\varphi^2$. For a particle of energy ε we seek solution of Eq. (1) in the form $\Psi(x) = e^{-i\varepsilon t}\psi(r)Y_{lm}(\theta, \varphi)$. Considering for simplicity the case of a massless particle in the s-wave ($l = 0$), one obtains the radial equation

$$\psi''(r) + \left(\frac{1}{r - r_s} + \frac{1}{r}\right)\psi'(r) + \frac{r^2\varepsilon^2}{(r - r_s)^2}\psi(r) = 0. \quad (3)$$

If the radius of the body R only slightly exceeds r_s, the first term in brackets dominates for $r - r_s \ll r_s$, and the solution just outside the body is the following linear combination of the incoming and outgoing waves,

$$\psi \sim \exp\left[-ir_s\varepsilon \ln\frac{r - r_s}{r_s}\right] + \mathcal{R}\exp\left[ir_s\varepsilon \ln\frac{r - r_s}{r_s}\right], \quad (4)$$

where $\mathcal{R}$ is the reflection coefficient. It is determined either by the boundary condition at $r = R$ (e.g., total absorption $\mathcal{R} = 0$ imposed for a black hole [3]), or by matching the solution with that at $r < R$ (e.g., analytically continuing to $r < r_s$ [8,9]).

At large distances $r \gg r_s$ Eq. (3) takes the form of the nonrelativistic radial Schrödinger equation for a particle of unit mass and momentum ε in the Coulomb-like potential Z/r with $Z = -\varepsilon^2 r_s$. For $\varepsilon r \gg 1$ its solution has the standard form

$$\psi \propto r^{-1}(e^{-iz} - Se^{iz}), \quad (5)$$

where $z = \varepsilon r + \varepsilon r_s \ln 2\varepsilon r$, which defines the scattering matrix S. To find S, one integrates Eq. (3) outwards starting from one of the exponential solutions in Eq. (4), which gives a linear combination of ingoing and outgoing waves at large r,

$$\exp\left[-ir_s\varepsilon \ln\frac{r - r_s}{r_s}\right] \rightarrow \frac{r_s}{r}\left[\alpha(\varepsilon)e^{-iz} + \beta(\varepsilon)e^{iz}\right], \quad (6)$$

where $|\alpha|^2 - |\beta|^2 = 1$ due to flux conservation. Comparison of Eqs. (4)–(6) gives the S matrix as

$$S = -\frac{\beta + \alpha^*\mathcal{R}}{\alpha + \beta^*\mathcal{R}}. \quad (7)$$

At low energies $\varepsilon r_s \ll 1$, α and β from Eq. (6) can be found by matching the Coulomb solutions valid at large distances with an intermediate-range solution obtained by neglecting the last term in Eq. (3) [10],

$$\alpha = \frac{i(1 + \varepsilon^2 r_s^2 C^2)}{2\varepsilon r_s C}\exp(-i\delta_C), \quad (8)$$

$$\beta = -\frac{i(1 - \varepsilon^2 r_s^2 C^2)}{2\varepsilon r_s C}\exp(i\delta_C), \quad (9)$$

where $C^2 = 2\pi\varepsilon r_s/[1 - \exp(-2\pi\varepsilon r_s)]$ and δ_C is the Coulomb phase shift [18].

B. Interior solution

Consider a massive body with radius $R > r_s$ and interior metric

$$ds^2 = a(r)dt^2 - b(r)dr^2 - r^2 d\Omega^2, \quad (10)$$

which matches that of Eq. (2) at the boundary: $a(R) = \xi$ and $b(R) = \xi^{-1}$, where $\xi = 1 - r_s/R$. For this metric the s-wave radial equation is

$$\frac{1}{r^2}\sqrt{\frac{a}{b}}\frac{d}{dr}\left(r^2\sqrt{\frac{a}{b}}\frac{d\psi}{dr}\right) + \varepsilon^2\psi = 0. \quad (11)$$

Its analysis is particularly simple if we change the radial wave function to $\phi = r\psi$, and the radial variable to the Regge-Wheeler "tortoise" coordinate r^* defined by $dr^* = \sqrt{b/a}\,dr$. This gives the following Schrödinger-like equation

$$\frac{d^2\phi}{dr^{*2}} + \left[\varepsilon^2 - \frac{1}{2r}\left(\frac{a}{b}\right)'\right]\phi = 0. \quad (12)$$

The second term in brackets plays the role of an effective potential for the motion in the r^* coordinate.

For a near-black-hole interior metric, $a(r) \rightarrow 0$ for $0 \le r \le R$, as the time slows down in the limit $\xi \rightarrow 0$. This means that the second term in brackets in Eq. (12) can be neglected for all except very small energies, and the solution describes free motion in the tortoise coordinate. The solution regular at the origin then is

$$\phi \simeq \sin\varepsilon r^* = \sin\left(\varepsilon\int_0^r \sqrt{\frac{b(r')}{a(r')}}dr'\right). \quad (13)$$

Matching this wave function to that of Eq. (3) at $r = R$ yields the reflection coefficient

$$\mathcal{R} = -\exp[2i\varepsilon r_s B(\xi)], \quad (14)$$

where

$$r_s B(\xi) = \int_0^R \sqrt{\frac{b(r)}{a(r)}}dr - r_s \ln\frac{R - r_s}{r_s}. \quad (15)$$

Here the first term is due to the large phase accumulated by the interior solution. It increases much faster than the second one, and dominates for $\xi \rightarrow 0$ where $B(\xi) \rightarrow \infty$. This large integral also gives the classical time that a massless particle ($ds^2 = 0$) spends in the interior. Its actual dependence on ξ depends on the model used for the interior metric (see Sec. III).

C. Scattering matrix and resonances

For $\xi \ll 1$, the scattering matrix S at low energies $\varepsilon r_s \ll 1$ is found explicitly using Eqs. (8) and (9) [10],

$$S = \frac{1 - \varepsilon^2 r_s^2 C^2 + (1 + \varepsilon^2 r_s^2 C^2)\mathcal{R}}{1 + \varepsilon^2 r_s^2 C^2 + (1 - \varepsilon^2 r_s^2 C^2)\mathcal{R}} \, e^{2i\delta_C}. \quad (16)$$

Since the phase $2\varepsilon r_s B(\xi)$ of $\mathcal{R}$ in Eq. (14) is large, one can show that the S-matrix has many poles close to the real energy axis at $\varepsilon = \varepsilon_n - i\gamma_n/2$ $(n = 1, 2, \dots)$. They correspond to resonances with positions and widths

$$\varepsilon_n = \frac{n\pi}{r_s B(\xi)}, \quad (17)$$

$$\gamma_n = \frac{2\varepsilon_n^2 r_s C^2}{B(\xi)} = \frac{2\pi^2 n^2 C^2}{r_s [B(\xi)]^3}. \quad (18)$$

While both ε_n and γ_n for a given n depend on ξ and tend to zero in the limit $R \to r_s$, the *ratio* of the width to the level spacing $D = \varepsilon_{n+1} - \varepsilon_n$,

$$\gamma_n/D = 2\varepsilon^2 r_s^2 C^2/\pi, \quad (19)$$

is independent of ξ for a given energy $\varepsilon_n \approx \varepsilon$.

Equation (19) shows that at low energies $\varepsilon r_s \ll 1$ the widths are much smaller than the resonance spacings. In this case the cross section for the capture of the particle into these long-lived states is described by the optical-model energy-averaged absorption cross section [18]

$$\bar{\sigma}_a^{\text{opt}} = \frac{2\pi^2}{\varepsilon^2} \frac{\gamma_n}{D}. \quad (20)$$

Substituting (19) into (20) yields

$$\bar{\sigma}_a^{\text{opt}} = 4\pi r_s^2, \quad (21)$$

which is equal to Unruh's low-energy absorption cross section for a black hole [3]. Note that this result does not depend on R or $B(\xi)$ for $\xi \ll 1$, that is, it is *independent* of the particular interior metric used.

D. Absorption cross section

More generally, the optical-model absorption cross section is defined as

$$\bar{\sigma}_a^{\text{opt}} = \frac{\pi}{\varepsilon^2}(1 - |\bar{S}|^2), \quad (22)$$

where the S matrix is averaged over an energy interval containing many resonances [18]. Without such averaging $|S| = 1$, as long as $|\mathcal{R}| = 1$ in Eq. (7), and the absorption cross section is zero.

For the near-black-hole metric $(\xi \to 0)$ the energy-averaging is equivalent to averaging S from Eq. (7) over the large phase $\Phi = \varepsilon r_s B(\xi)$ of the reflection coefficient $\mathcal{R} = -e^{2i\Phi}$. Since α and β have a much slower dependence on ε than Φ, this gives

$$\bar{S} = -\frac{1}{\pi} \int_0^\pi \frac{\beta - \alpha^* e^{2i\Phi}}{\alpha - \beta^* e^{2i\Phi}} d\Phi = -\frac{\beta}{\alpha}. \quad (23)$$

Hence, we see that averaging over the large phase Φ is equivalent to setting $\mathcal{R} = 0$ in Eq. (7), that is, to the

assumption that there is no outgoing wave in Eq. (4) in the vicinity of the horizon.

At low energies $\varepsilon r_s \ll 1$, the scattering matrix, $S = \exp[2i(\delta_C + \delta)]$, and the corresponding short-range scattering phase shift δ display narrow resonances (see Sec. III). The lifetime of these resonances (γ_n^{-1}) is related to the derivative of the phase shift $d\delta/d\varepsilon$ taken at the resonance, and is large for $\xi \to 0$. More generally, in quantum mechanics, this derivative corresponds to the expectation value of the *time delay* caused by trapping of the particle in the potential well [21].

At higher energies, $\varepsilon r_s \gtrsim 1$, the quantum resonances become broad, and the motion becomes semiclassical. In this regime the phase shift δ is determined by the large (semiclassical) phase of the internal wave function in Eq. (13). The corresponding quantum delay time is then given by the classical dilation time $\int_0^R \sqrt{b(r)/a(r)} dr$, which also tends to infinity for $\xi \to 0$.

The long trapping that one observes in the limit $R \to r_s$ at both low and high energies provides a physical explanation for the no-reflection condition $\mathcal{R} = 0$ that emerges as a result of averaging of the scattering matrix in Eq. (23).

III. EXAMPLES OF INTERIOR METRIC

In this section we illustrate our findings using particular models of the interior metric. The standard Schwarzschild interior solution for a sphere of constant density develops a pressure singularity when $r_s = 8R/9$ [22]. This forbids the investigation of the black-hole limit $R \to r_s$ in this model. Examples of interior metric free from such singularity were proposed by Florides [20,23]

$$a(r) = \frac{(1 - r_s/R)^{3/2}}{\sqrt{1 - r_s r^2/R^3}}, \qquad b(r) = \left(1 - \frac{r_s r^2}{R^3}\right)^{-1}, \quad (24)$$

and Soffel *et al.* [14], for which

$$a(r) = \left(1 - \frac{r_s}{R}\right)\exp\left[-\frac{r_s(1 - r^2/R^2)}{2R(1 - r_s/R)}\right], \quad (25)$$

and $b(r)$ is given by Eq. (24). Both metrics are valid for $0 \le r \le R$ for any $R > r_s$, and match the Schwarzschild solution at $r = R$.

A. Florides metric

For the Florides metric, using $a(r)$ and $b(r)$ from Eq. (24), we solve the second-order differential equation (11) numerically with the boundary condition $\psi(0) = 1$, $\psi'(0) = 0$ using *Mathematica* [24]. This solution provides a real boundary condition for the *exterior* wave function at $r = R$. (We set $R = 1$ in the numerical calculations). Equation (3) is then integrated outwards to large distances $r \gg r_s$. In this region Eq. (3) takes the form of a nonrelativistic Schrödinger equation for a particle with momentum ε and unit mass in the Coulomb potential
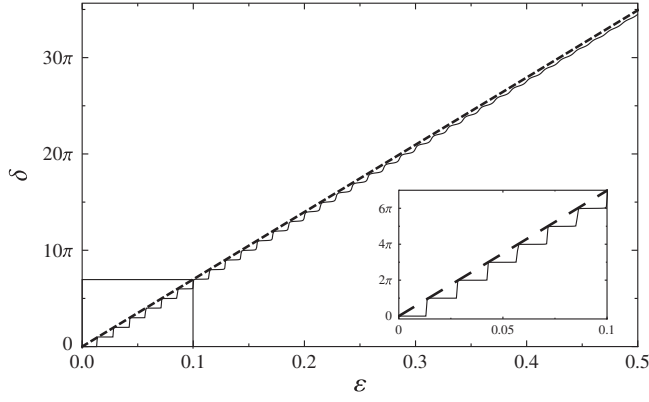
FIG. 1. Short-range phase shift δ as a function of energy obtained numerically for $r_s = 0.999R$ (solid line). The dashed line shows the phase accumulated by the wave function at $r \leq R$, $\Phi = \varepsilon r_s B(\xi)$, see Eqs. (13), (15), and (28).

FIG. 3. Dependence of the energy ε_n (main plot) and width γ_n (inset) of the $n = 6$ resonance on r_s for the Florides interior metric. Solid circles show the numerical values and solid lines show the results obtained from Eqs. (17) and (18) using $B(\xi)$ from Eq. (28).

with charge $Z = -r_s \varepsilon^2$. Hence, we match the solution with the asymptotic form [18]

$$\psi(r) \propto \sin[\varepsilon r - (Z/\varepsilon)\ln 2\varepsilon r + \delta_C + \delta] \qquad (26)$$

where $\delta_C = \arg\Gamma(1 + iZ/\varepsilon)$ is the Coulomb phase shift, and determine the short-range phase shift δ.

The phase shift δ is due to the interior metric, and it carries information about the behavior of the wave function at $r \leq R$. Unlike δ_C which is small and has a weak dependence on the energy, δ depends strongly on the energy of the particle, and is large for r_s close to R (i.e., for $\xi \ll 1$). This is shown in Fig. 1 for $r_s = 0.999R$ (solid line). The phase shift δ goes through many steps of the size π, which correspond to the resonances described in Sec. II. They occur approximately where the phase $\Phi = \varepsilon r_s B(\xi)$ of the interior solution equals $n\pi$. For the Florides metric the phase integral in Eq. (15) is

$$\int_0^R \sqrt{\frac{b}{a}}dr = \int_0^R \frac{\xi^{-3/4}dr}{\sqrt[4]{1 - r_s r^2/R^3}} \simeq Ar_s\xi^{-3/4}, \qquad (27)$$
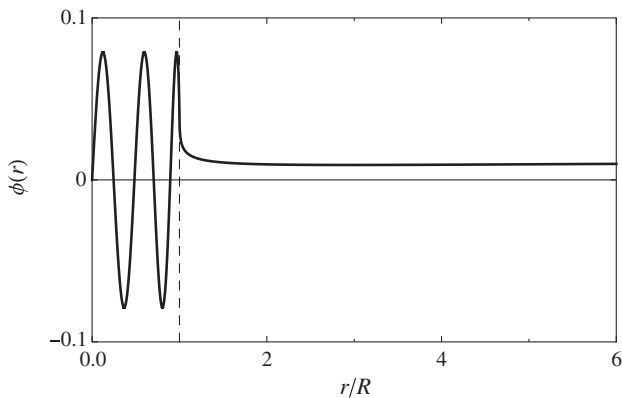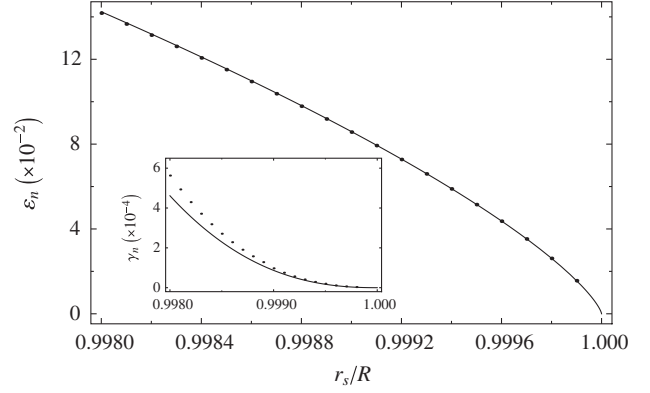
where $A = \sqrt{\pi}\Gamma(3/4)/[2\Gamma(5/4)] \approx 1.198$, so that

$$B(\xi) = A\xi^{-3/4} - \ln\xi. \qquad (28)$$

The corresponding phase Φ is shown in Fig. 1 by the dashed line. Apart from the resonant steps, it matches closely the short-range phase shift from the numerical calculation.

For the "on-resonance" energies corresponding to the midpoints of the steps (where $d\delta/d\varepsilon$ is largest) the magnitude of the wave function $\phi(r)$ inside the body ($r < R$) is much greater than outside. This is a signature of a quasi-stationary state of the trapped particle, and is shown in Fig. 2.

The phase obtained using the Florides interior metric, Eq. (27), shows that the time dilation effect for the particle inside the massive body, $d\delta/d\varepsilon$, increases as $(R - r_s)^{-3/4}$. The lifetimes of the resonances are in fact even longer. As already mentioned in Sec. II, the rapid variation of the phase of $\mathcal{R}$ with energy gives rise to a sequence of resonant
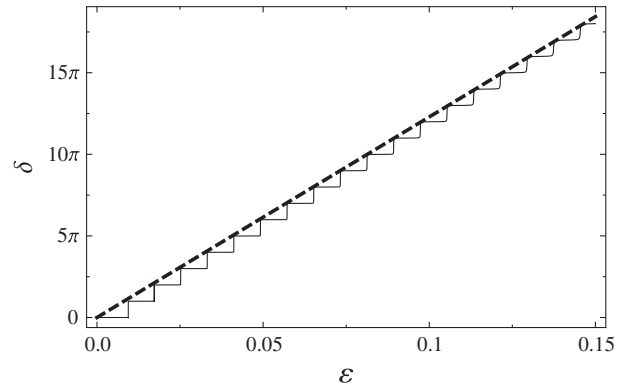

FIG. 2. Radial wave function $P(r) = r\psi(r)$ of the fifth resonance, $\varepsilon \approx 0.071$, for $r_s = 0.999R$.

FIG. 4. Short-range phase δ obtained for the Soffel interior metric for $r_s/R = 0.955$ (solid line), and the interior phase $\Phi = \varepsilon r_s B(\xi)$ (dashed line), with $B(\xi)$ given by Eq. (30).
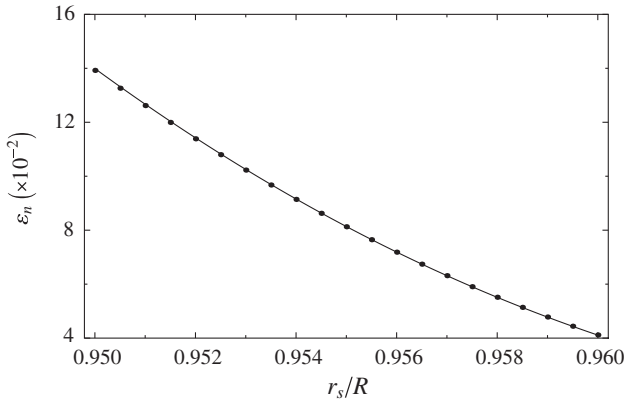
FIG. 5. Energy of the $n = 10$ resonance obtained for the Soffel interior metric as a function of r_s: solid circles—numerical values; solid line—analytical result, Eqs. (17) and (30).

FIG. 6. Width of the $n = 10$ resonance obtained for the Soffel interior metric as a function of r_s: solid circles—numerical values; solid line—analytical result, Eqs. (18) and (30).

poles in the S-matrix. The energies and widths of the resonances are described by Eqs. (17) and (18), respectively. Numerically, they can be determined by fitting the "steps" in δ with $\arctan[2(\varepsilon - \varepsilon_n)/\gamma_n]$ [18].

Figure 3 shows that the dependence of the resonance energy and width on r_s obtained numerically and analytically are in good agreement. In particular, we observe the rapid vanishing of the width $\gamma_n \propto (R - r_s)^{9/4}$ predicted by Eqs. (18) and (28). Therefore, numerical calculation using the Florids metric fully confirm the general analysis of the scattering problem presented in Sec. II.

B. Soffel metric

To verify our conclusions, we have also investigated the scattering problem for r_s close to R using the Soffel interior metric, Eq. (25). We do this numerically using *Mathematica*, as described in Sec. III A. The corresponding short-range scattering phase shift δ is shown in Fig. 4 for $r_s = 0.955R$. It displays resonance steps similar to those in Fig. 1.

For the Soffel metric the leading contribution to the interior wave function phase Φ is

$$\int_0^R \sqrt{\frac{b}{a}} dr = \int_0^R \frac{\exp[r_s(1 - r^2/R^2)/(4R\xi)]}{\sqrt{\xi(1 - r_s r^2/R^3)}} dr, \quad (29)$$

which for $\xi \ll 1$ gives [cf. Eq. (28)]

$$B(\xi) \simeq \sqrt{\frac{\pi}{1 - 3\xi}} \exp\left(\frac{1 - \xi}{4\xi}\right) - \ln\xi. \quad (30)$$

This expression shows that for the Soffel metric the short-range phase δ, the resonance level density and their lifetimes increase exponentially for $r_s \to R$, i.e., for $\xi \to 0$. This explains why in the Soffel metric the onset of the resonant scattering picture similar to that seen in the Florides metric occurs earlier, i.e., at smaller values of
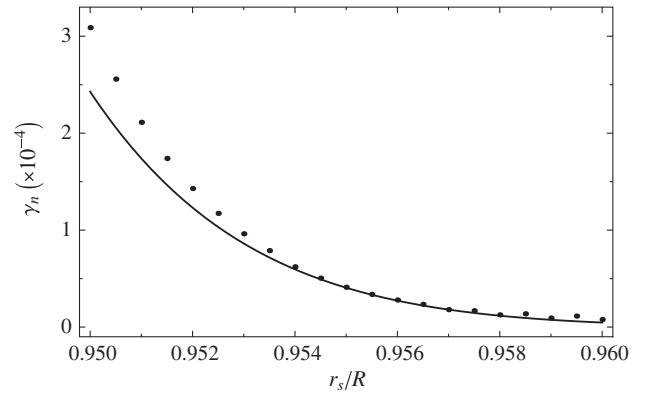
r_s/R. We see that the dependence of $B(\xi)$, Φ and the short-range phase δ on ξ is not inversal. However, the dependence of the short-range phase and resonances on the large parameter $B(\xi)$ [$B(\xi) \to \infty$ for $\xi \to 0$], Eqs. (16)–(18), is universal.

Figure 5 shows the dependence of the resonance energy ε_n on r_s/R for $n = 10$. It also shows that the numerical values obtained by fitting the short-range phase with the resonant profile $\arctan[2(\varepsilon - \varepsilon_n)/\gamma_n]$ (shown by circles), are in good agreement with those obtained from Eqs. (17) and (30) (solid line).

As in the case of the Florides metric, the resonance widths γ_n display a much faster decrease than the energies ε_n for $r_s \to R$. This is shown for $n = 10$ in Fig. 6. The strong dependence of γ_n on r_s/R is explained by the rapid (exponential) increase of $B(\xi)$ with decreasing ξ, see Eqs. (18) and (30).

Hence, we see that the picture of resonant scattering for a metric close to the black-hole limit, is independent of the particular interior metric used.

IV. CONCLUSIONS

The problem of scattering of low-energy scalar particles from a massive static spherical body has been considered. We have shown that as the black-hole metric limit is approached, a dense spectrum of long-lived resonances emerges in the problem. Long-time-delay trapping of the particles in these resonances gives rise to effective absorption in a purely potential scattering problem. We are grateful to the anonymous referee for the important observation that the existence of the narrow resonances may be linked to the "no-hair" theorem, as the particle must be trapped inside in the limit $R = r_s$.

This shows that the absorption boundary condition ($\mathcal{R} = 0$) emerges naturally in the limit $R \to r_s$, as a result of particle capture into the dense spectrum of long-lived resonances.

[1] R. A. Matzner, J. Math. Phys. (N.Y.) **9**, 163 (1968).
[2] A. A. Starobinskii, Zh. Eksp. Teor. Fiz. **64**, 48 (1973) [Sov. Phys. JETP **37**, 28 (1973)].
[3] W. G. Unruh, Phys. Rev. D **14**, 3251 (1976); thesis, Princeton University, 1971 (unpublished).
[4] N. Sanchez, Phys. Rev. D **18**, 1030 (1978).
[5] S. R. Das, G. Gibbons, and S. D. Mathur, Phys. Rev. Lett. **78**, 417 (1997).
[6] L. C. B. Crispino, S. R. Dolan, and E. S. Oliveira, Phys. Rev. Lett. **102**, 231103 (2009).
[7] Y. Décanini, G. Esposito-Farèse, and A. Folacci, Phys. Rev. D **83**, 044032 (2011).
[8] M. Yu. Kuchiev, Europhys. Lett. **65**, 445 (2004).
[9] M. Yu. Kuchiev, Phys. Rev. D **69**, 124031 (2004).
[10] M. Yu. Kuchiev and V. V. Flambaum, Phys. Rev. D **70**, 044022 (2004).
[11] C. V. Vishveshwara, Nature (London) **227**, 936 (1970).
[12] N. Deruelle and R. Ruffini, Phys. Lett. B **52**, 437 (1974).
[13] T. Damour, N. Deruelle, and R. Ruffini, Lett. Nuovo Cimento **15**, 257 (1976).
[14] M. Soffel, B. Müller, and W. Greiner, J. Phys. A **10**, 551 (1977).
[15] D. W. Pravica, Proc. R. Soc. A **455**, 3003 (1999).
[16] K. Glampedakis and N. Andersson, Classical Quantum Gravity **20**, 3441 (2003).
[17] J. Grain and A. Barrau, Eur. Phys. J. C **53**, 641 (2008).
[18] L. D. Landau and E. M. Lifshitz, *Quantum Mechanics* (Butterworth-Heinemann, Oxford, 1977), 3rd ed..
[19] G. H. Gossel, J. C. Berengut, and V. V. Flambaum, Gen. Relativ. Gravit. **43**, 2673 (2011).
[20] To avoid misunderstanding, we should note that the Florides metric does not correspond to any macroscopic object for $R < 3r_s/2$, but may represent the gravitational field inside a cluster of particles moving in randomly oriented circular orbits for larger R. This is further discussed by N. K. Kofinti, Gen. Relativ. Gravit. **17**, 245 (1985); L. Herrera and N. O. Santos, Phys. Rep. **286**, 53 (1997).
[21] F. T. Smith, Phys. Rev. **118**, 349 (1960).
[22] H. A. Buchdahl, Phys. Rev. **116**, 1027 (1959).
[23] P. S. Florides, Proc. R. Soc. A **337**, 529 (1974).
[24] Wolfram Research, Inc. *Mathematica, Version 7.0* (Wolfram Research, Inc., Champaign, IL, 2008).